DE GRUYTER OPEN

ADVANCES IN MANUFACTURING SCIENCE AND TECHNOLOGY
Vol. 40, No. 2, 2016
DOI: 10.2478/amst-2016-0010

THE POROSITY ASSESSMENT OF CERAMIC TOPCOAT IN THERMAL BARRIER COATINGS DEPOSITED BY APS METHOD

Maciej Pytel, Marek Góral, Andrzej Nowotnik

Summary

In the paper the comparison of open porosity measurement results of ceramic topcoats in thermal barrier coatings (TBCs) was presented. TBCs were produced by Air Plasma Spraying (APS) method and were consisted of two coatings – an outer ceramic topcoat and metallic MeCrAlY bond coat deposited onto surface of René80 Ni-based superalloy. For deposition of ceramic coatings Metco 201 B NS, Metco 204 NS and Metco 210 powders were used whereas for deposition of metallic bond coat AMDRY 365-1 MeCrAlY powder was used. Both types of coatings were deposited using Thermico A60 plasma gun. The microstructure investigations of cross-sections of produced TBC's were carried out using Hitachi S-3400N scanning electron microscope. Qualitative image analysis of microstructure of produced TBCs as well as analysis of percentage of pores surface area content A_A was performed. The evaluation of porosity in ceramic topcoat was carried out by image analysis using MeTilo v.12.1 quantitative software.

Keywords: Air Plasma Spraying (APS), MeCrAlY bond coats, ceramic topcoats, porosity of TBCs

Ocena porowatości warstwy ceramicznej powłokowej bariery cieplnej (TBC) wytworzonej w procesie natryskiwania plazmowego (APS)

Streszczenie

W pracy przedstawiono analizę wyników badań porowatości otwartej w zewnętrznej warstwie ceramicznej powłokowej bariery cieplnej TBC. Międzywarstwę metaliczną wytworzono przy użyciu proszku AMDRY 365-1, natomiast warstwę ceramiczną przy zastosowaniu proszku Metco 201 B NS, Metco 204 NS i Metco 210 firmy Oerlikon Metco. Warstwy natryskiwano za pomocą jednoelektrodowego palnika plazmowego A60 firmy Thermico, w warunkach ciśnienia atmosferycznego (APS) na podłożu nadstopu niklu René 80. Badania mikroskopowe powłokowych barier cieplnych TBC prowadzono przy użyciu skaningowego mikroskopu elektronowego Hitachi S-3400N. Wykonano analizę jakościową obrazów mikrostruktury oraz określono pole powierzchni przekroju płaskiego porów otwartych. W ocenie porowatości zewnętrznej warstwy ceramicznej stosowano program komputerowy do ilościowej analizy obrazu MeTilo v.12.1.

Słowa kluczowe: natryskiwanie plazmowe APS, międzywarstwa MeCrAlY, zewnętrzna warstwa ceramiczna $ZrO_2xY_2O_3$, porowatość warstwy ceramicznej

Address: Maciej PYTEL, PhD Eng., Marek GÓRAL, PhD Eng., Andrzej NOWOTNIK, PhD Eng., Rzeszów University of Technology, Department of Materials Science, 8 Powstańców Warszawy Av., 35-959 Rzeszów, e-mail: mpytel@prz.edu.pl, mgoral@prz.edu.pl

1. Introduction

Thermal Barrier Coatings (TBCs) can be produced using various methods, i.e. APS – Air Plasma Spraying, LPPS PS-PVD – Low Pressure Plasma Spay/Plasma Spray-Physical Vapor Deposition or EB-PVD – Electron Beam-Physical Vapor Deposition. Generally are consisted of two types of coatings, an outer ceramic topcoat and metallic bond coat. Ceramic topcoats are deposited on various types of bond coats but mostly on MeCrAlY bond coats deposited by Air Plasma Spraying method or on diffusion aluminide coatings deposited by, e.g. CVD method [1-6].

TBC's form a composite structure and are consisted of at least two coatings where each of them plays a different role due to its different chemical and phase composition and properties, e.g. the outer ceramic coating (top coat) made from yttria stabilized zirconia (YSZ) powders or ingots plays a role of thermal insulation which lowers the base material temperature by up to 200°C. Between the outer coating and substrate material (most common Ni-based superalloy) occurs a bond coat, which protects the substrate from high temperature oxidation or hot corrosion. A compensation for mechanical and thermal stresses is also a role of these coatings (resulting from different coefficients of linear thermal expansion α and thermal conductivity γ between Ni-based superalloy and the ceramic coating) [7]. Bond coats are mostly diffusion coatings, while thermal barrier coatings are attached to the substrate surface by adhesion strength (YSZ-APS) or by a bonding to the TGO zone (thermally grown oxide), e.g. in EB-PVD TBC system, however the bonding mechanism of these coatings remains a subject of continuous research [8-11]. Various methods of producing TBC coatings determine their structure, which influences their properties. This, in turn, influences their application. EB-PVD TBC-type coatings can be successfully applied on rotating elements in the hot section of the jet engine or in stationary gas turbines, whereas APS TBC-type coatings are most often used on stationary elements, combustion chambers, vanes etc. This results from their structure and properties as presented in Table 1.

Differences in structure of APS and EB-PVD TBC systems TBC's are the cause of differences in their porosity [1,12]. In PS-PVD or EB-PVD TBC coatings with columnar structure of ceramic topcoat a gradient porosity can be observed, that is porosity values vary on the cross-section from the surface towards the substrate. In TBC coatings such as EB-PVD type an inter-columnar gaps, intra-columnar micro-pores or nanopores are observed [13,14]; its value varies from the substrate (e.g. surface of bond coat) towards the outer surface due to the fact that columns are more narrow at the base (bond coat) (where they have been deposited) and then become wider towards the outer surface. An example of analysis of intercolumnar porosity in EB-PVD TBC coatings was presented by Kelly M., Singh J. et al [15]. In TBC coatings deposited by APS method the porosity can be open and closed, however only open (or interlamellar) porosity can be observed and measured using microscopic methods. Open pores seen as darker areas are

only a part of the total porosity, and their flat surface area is a relative value of the total porosity of these TBCs.

Table 1. Comparison of basic microstructure characteristics of EP-PVD and APS TBCs

Coating	Characteristics
EP-PVD	Columnar microstructure, Excellent tolerance to thermal stresses, Required careful preparation of the Bond Coat surface to obtain good quality of the YSZ coating, YSZ ceramic coating is attached to the TGO oxide layer (Al_2O_3), Deposition occurs above 900 °C
APS	Porous, lamellar microstructure, Good tolerance to stresses due to porosity and subcritical microcracks, Required coarse surface of the bond coat for good mechanical adhesion of the YSZ coating, deposition occurs below 300 °C

Due to the fact that these coatings differ in their microstructure and complex structure, and also because of their composite character, a number of metallographic techniques for preparing microsections for microstructure examination are required. In order to determine their porosity, distribution and oxide shape, and to differentiate them from pores, various of microstructure observation techniques are used, e.g. with the use of light microscope (LM) or scanning electron microscope (SEM).

The presence of pores in TBCs is one of the most important characteristics of TBCs which affects many of their properties, i.e. affects the thermal diffusivity and conductivity, allows the compensation of thermo-mechanical stresses. Therefore, an important aspect is to apply an appropriate methodology for metallographic sample preparation and subsequent image analysis of TBC coatings in order to carry out a thorough evaluation of porosity [16-18].

To render a good quality image of the microstructure of complex coatings such as TBC with use of light microscope (metallographic), a number of conditions must be fulfilled. First and foremost, the microsection surface must be even, clean and free from impurities, and pores must be well exposed. Even if the microsection of TBC coatings has been made properly, it is difficult with use of an light microscope (LM) to render a good depth of field of the image, contrast and evenly distributed lighting due to differences in optical properties of ceramic coating and metallic substrate (bond coat or base material). Ceramics then gives a dark image, while metal is illuminated too strongly.

This makes contrast and image focus quite difficult to render. The problem can be solved through combination of proper preparation and use of a scanning electron microscope for microstructure examination, which deliver good results.

Images rendered by SEM have higher resolution than LM, are focused, sharper, well illuminated and display a good depth of field. It also enables the EDS

analysis (also X-ray EDS mapping) of chemical composition of individual microstructure constituents, e.g. determining whether a given constituent is an oxide or other inclusion, which can often be mistaken. Image manipulation is also possible (observation parameters can be amended, just as sample current, acceleration voltage etc.) in order to distinguish a particular constituent of the microstructure.

2. Examinations

The aim of the study was to determine the value of porosity of the ceramic coatings in the produced APS TBC coatings. The percentage of the surface area of pores A_A in the analyzed image of the microstructure of produced TBC coatings was measured. Qualitative assessment of the micrographs of TBCs microstructure was also conducted. As the research material René 80 polycrystalline Ni-based superalloy (GE trademark) was choosen. Both the metallic bond coats and the ceramic topcoats were deposited onto René 80 surface using Thermico A60 plasma gun by APS method. The metallic bond coats were prepared as the first. All the metallic bond coats were deposited with use of AMDRY 365-1 metallic MeCrAlY powder: Ni in balance,18-28 wt.% of Co, 13-21 wt.% of Cr, 10-15 wt.% of Al, 0.1-0.8 wt.% of Y and other element $\leq$ 5.0 wt.% then onto their surface ceramic topcoats with use of Metco 201 B NS, 204 NS and 210 ceramic powders by Oerlikon Metco (formerly Sulzer Metco) were deposited of which the chemical composition was presented in the Table 2 [19]. As the plasma gases argon and hydrogen was used and their flow rate amounted to 70 dm^3/min, current intensity was 500A and flow rate of powders was 15 g/min. The distance from the source to the René 80 surface was 100 mm.

Table 2. Chemical composition of ceramic powders applied for deposition of Thermal Barrier Coatings by APS method – provided by manufacturers

Powder type	**Chemical composition, wt.%**								
	ZrO_2	Y_2O_3	CaO	MgO	Al_2O_3	SiO_2	TiO_2	Fe_2O_3	Other oxides
Metco 201 B NS	91.5		4.5 -5.5						3.0 -4.0
Metco 204 NS	89.7 -91.7	7.0 -9.0	-	-	max. 0.2	max. 0.7	max. 0.2	max. 0.2	-
Metco 210	~93.0			15.0 -30.0					max. 7.0

The metallographic samples were mounted in epoxy resin and also in Struers Polyfast thermosetting resin (electrically conducted). The microsections were

prepared in accordance with the procedure as shown in Table 4. This method is faster than a standard methodology for metallographic sample preparation (Table 3). Microstructural examinations were carried out using Hitachi S3400N

Table 3. Standard methodology for preparation of metallographic specimens

Step no.	Paper/Disc/Cloth	Abrasive type/ size	Lubricant/ Coolant	Force per sample, N	Speed, RPM	Time, s
1	Paper	120	Water	35	300	60
2	Paper	220	Water	35	300	60
3	Paper	320	Water	35	300	60
4	Paper	500	Water	35	300	60
5	Paper	600	Water	35	300	60
6	Paper	800	Water	35	300	60
7	Paper	1000 or next 2400	Water	35	300	60
8	MD-Mol/Nap	3 µm diamond suspension	Green coolant	15-25	150	120-240
9	MD-Mol/Nap	1 µm diamond suspension	Green coolant	15-25	150	120-240
10*	MD-Chem	colloidal silica OP-S/U or alumina OP-AN/AA	Distilled water	10	150	60-120
Polishing surface and sample rotate (1-9) can be in the same direction						

*not always necessary

Table 4. Modified method for APS TBCs microsections preparation used in this research

Step no.	Paper/Disc/Cloth	Abrasive type/ size	Lubricant/ Coolant	Force per sample, N	Speed, RPM	Time, s
1	Paper	120/220*	Water	35	350	60
2	Paper	320	Water	35	350	60
3	Diamond grinding disc	9µm	Green coolant	35	350	240
4	MD-Mol	3 µm diamond suspension	Green coolant	20-25	150	120-240
5	MD-Mol/Nap	1 µm diamond suspension	Green coolant	15	150	120-240
6*	MD-Chem	colloidal silica OP-S/U or alumina OP-AN/AA	Distilled water	10	150	60-120

*not always necessary

scanning electron microscope. Samples for SEM examinations which were mounted in epoxy resin in the next step were gold sputter coated with the use of a High-Vacuum Cressington 108 Sputter Coater. Image recording for microstructure of examined coatings was carried out at 200x magnification and area of measurement was 100x500 µm. For porosity analysis MeTilo v.12.1 software was used [20, 21]. All testing and processes were performed in Department of Materials Science and in The Research and Development Laboratory for Aerospace Materials, which is an independent department located in Department of Materials Science within the Faculty of Mechanical Engineering and Aeronautics at Rzeszow University of Technology in Poland.

3. Results

The results of the SEM microstructure examinations of APS TBCs showed a typical structure for such coating as seen in Fig. 1-4. It was found that the microstructure is lamellar, dense and is characterized by many areas of elongated pores as well as the pores of the spherical shape as seen in Fig. 5-7. The coatings were also characterized by high surface roughness, and their thickness was different as shown in Table 5.

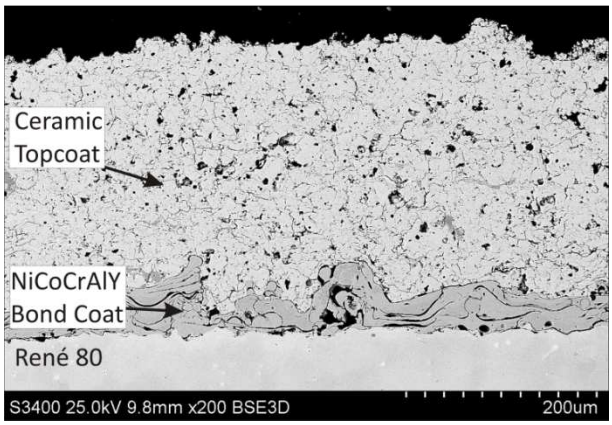

Fig. 1. Microstructure of APS TBC deposited using a Metco 201 B NS powder (ceramic top coat) onto AMDRY 365-1 NiCoCrAlY (bond coat) surface and René 80 substrate (mounted in epoxy resin)

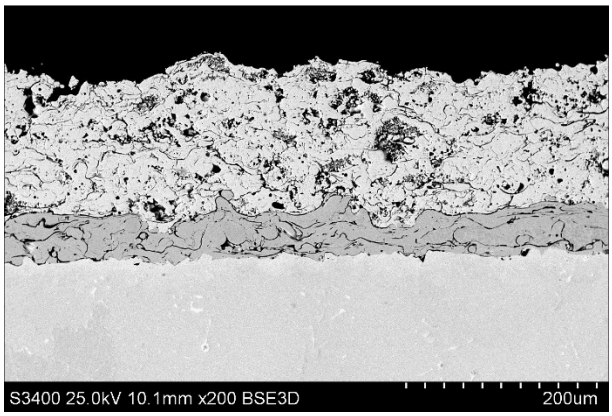

Fig. 2. Microstructure of APS TBC deposited using a Metco 204 NS powder (ceramic top coat) onto NiCoCrAlY (bond coat) surface and René 80 substrate (mounted in thermosetting resin)

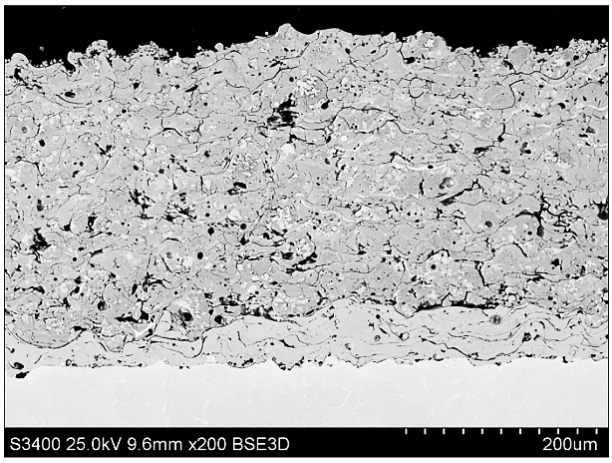

Fig. 3. Microstructure of APS TBC deposited using a Metco 210 powder (ceramic top coat) onto NiCoCrAlY (bond coat) surface and René 80 substrate (mounted in thermosetting resin)

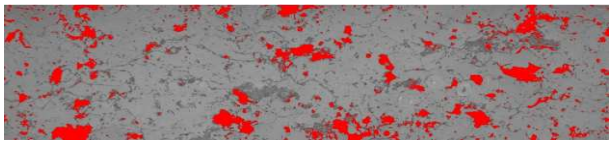

Fig. 4. An example of an incomplete detection of image detail (pores) due to inadequate lightning of sample

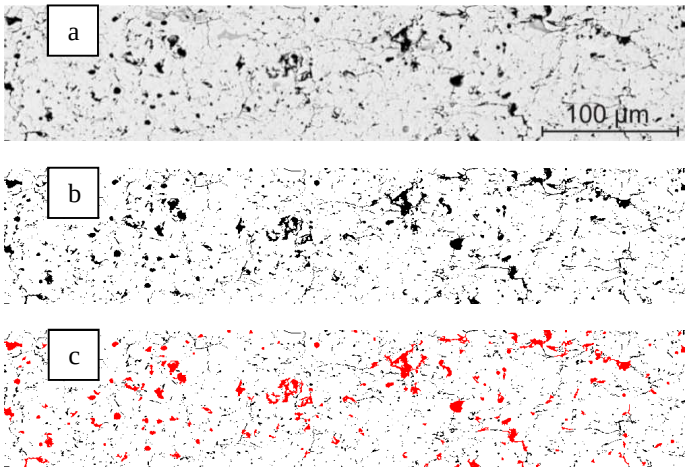

Fig. 5. Microstructure of Metco 201 B NS APS-TBC – a part of the image chosen for porosity analysis: a) BSE-SEM image; b) after binarization procedure; c) after complete image analysis procedure

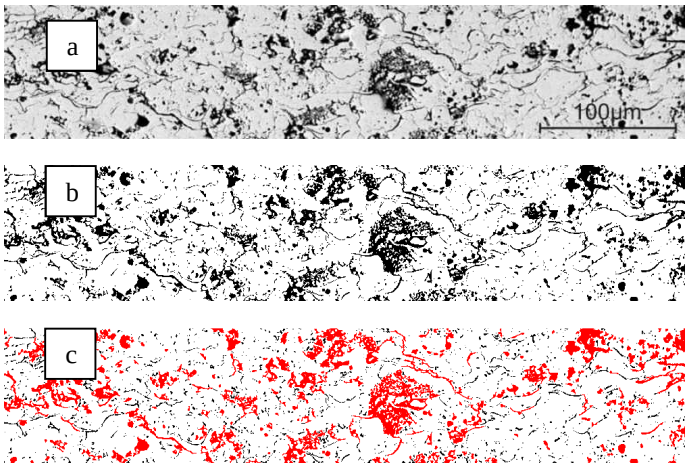

Fig. 6. Microstructure of Metco 204 NS APS-TBC – a part of the image chosen for porosity analysis: a) BSE-SEM image; b) after binarization procedure; c) after complete image analysis procedure

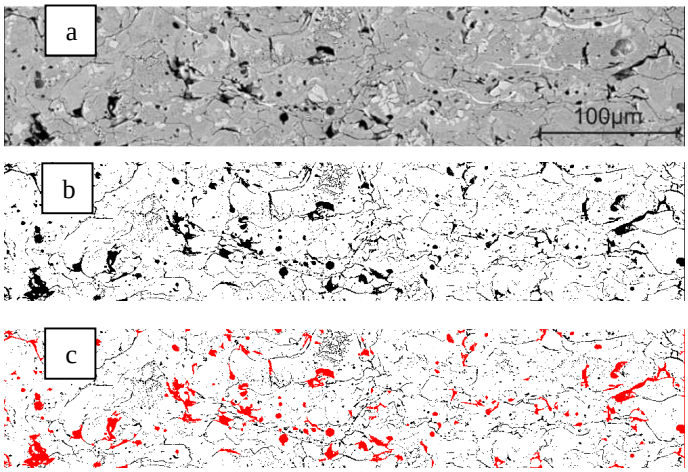

Fig. 7. Microstructure of Metco 210 APS-TBC – a part of the image chosen for porosity analysis: a) BSE-SEM image; b) after binarization procedure; c) after complete image analysis procedure

Table 5. Measurements of thickness of each coatings forming APS TBC

No.	Material/ type of coating	Average Thickness, µm	St Dev, µm
1	Metco 201 B NS/ceramic top coat AMDRY 365-1/bond coat	258 47	22 15
2	Metco 204 NS/ceramic top coat AMDRY 365-1/bond coat	150 43	10 9
3	Metco 210/ceramic top coat AMDRY 365-1/bond coat	286 38	14,9 17

Table 6. The results of measurement of the percentage of surface area of pores A_A in ceramic topcoat in APS TBC

Surface area of pores	Material/type of coating		
	APS ceramic topcoat		
	Metco 201 B NS	Metco 204 NS	Metco 210
A_A, %	4.0*	14.3*	5.9*
	4.7**	14.0**	6.0**

*mounted in epoxy resin: BSE-SEM low-vacuum mode at 30 Pa + gold sputtered, **mounted in thermosetting bakelite-BSE-SEM + gold sputtered

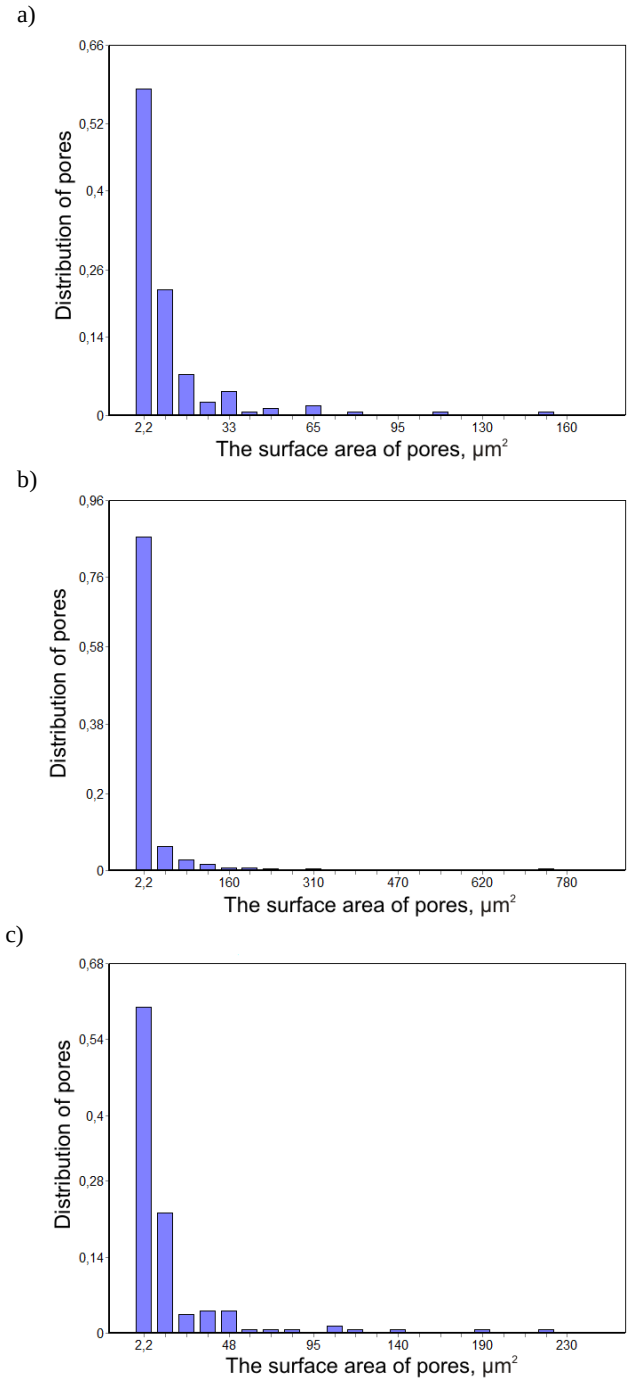

Fig. 8. The pores distribution as a function of their surface area measurements for APS ceramic topcoat produced using ceramic powders: a) Metco 201 B NS, b) Metco 204 NS and c) Metco 210

The total number of detected objects in analyzed image was 165 for Metco 201 B NS, 253 for Metco 204 NS and 145 for Metco 210 APS ceramic coating. Minimum measured surface area of pores was 2.21 μm^2 for Metco 201 B NS, 2.22 μm^2 for Metco 204 NS, 2.23 μm^2 for Metco 210. An average value of surface area of pores was 14.2 μm^2 for Metco 201 B NS , 27.5 μm^2 for Metco 204 NS and 21.1 μm^2 for Metco 210 while the maximum surface area of pores was 157 μm^2 for Metco 201 B NS, 774 μm^2 for Metco 204 NS and 233 μm^2 for Metco 210 APS TBC ceramic coatings as seen in Fig. 8.

4. Conclusions

On the basis of microstructural examinations of produced APS TBC coatings including qualitative and quantitative image analysis of their microstructure and porosity measurements it has been found that there are differences in the percentage of the pores surface area content in ceramic topcoats. Metco 201 B NS ceramic topcoat is characterized by the lowest (~4%) porosity among the studied coatings, the porosity of the Metco 210 ceramic topcoat was about 6% and for the Metco 204 N porosity was the highest and was 14% as shown in Table 6. The microstructural examinations of porous ceramic coatings of APS TBCs showed also that the use of BSE-SEM mode and low vacuum mode at 30 Pa and sputtering a thin layer of gold onto TBCs microsections surface gives good results in imaging of microstructure of TBCs for samples mounted in epoxy resin while for APS TBC samples mounted in thermosetting and electrically conductive resin, in a high vacuum mode, sputtering a thin layer of gold is sufficient. Vacuum sputtering a thin layer of gold allows for the improvement of image quality especially for the samples mounted in epoxy resin. It was found that the use of the proposed research methodology enables precise image analysis and evaluation of porosity of ceramic topcoat in APS TBC. Additionally the modified metallographic methodology of TBC microsections enables to reduce different types of artifacts and differentiate them from pores.

Microscopic examination of TBC coatings with use of SEM in the BSE or BSE3D modes renders very good results. Limitations which results from the electrical conductivity of YSZ ceramic coatings and metallic substrate can be avoided through sputter coating of a thin layer of gold onto the surface of microsection using vacuum sputter coater (glow discharge technique). Most commonly samples are mounted in epoxy resin (cold mounting) or in electrically conducting bakelite (hot mounting - at 150-180°C, 25 kN), which in turn can cause some limitations in image rendering (SEM), especially in the SE mode. In some cases hot press mounting of TBC's causes destruction of microsections due to spallation of the ceramic coating. Cold mounting in epoxy resin with gold sputtering technique can significantly reduce these limitations.

References

[1] Y. TAMARIN: Protective coatings for turbine blades. ASM International, Materials Park, 2002, OH 44073–0002.

[2] K. VON NIESSEN, M. GINDRAT: Plasma Spray-PVD: A new thermal spray process to deposit out of the vapor phase. *Journal of Thermal Spray Technology*, **20**(2011)4, 736-743.

[3] A. MARICOCCHI, A. BARTZ, D. WORTMAN: PVD TBC Experience on GE Aircraft Engines. *Journal of Thermal Spray Technology*, **6**(1997)2, 193-198.

[4] Y. ZHANG, W.Y. LEE, J.A. HAYNES, I.G. WRIGHT, B.A. PINT, K.M. COOLEY, and P.K. LIAW: Synthesis and cyclic oxidation behavior of a (Ni, Pt) Al coating on a desulfurized Ni-base superalloy. *Metallurgical and Materials Transactions A*, **30A**(1999), 2679-2687.

[5] S.J. HONG, G.H. HWANG, W.K. HAN, S.G. KANG: Cyclic oxidation of Pt/Pd-modified aluminide coating on a nickel-based superalloy at 1150 °C. *Intermetallics*, **17**(2009), 381-386.

[6] G. MOSKAL: Thermal barrier coatings: characteristics of microstructure and properties, generation and directions of development of bond. *Journal of Achievements in Materials and Manufacturing Engineering*, **37**(2009)2, 323-331.

[7] J. CHENG, E. H. JORDAN, B. BARBER and M. GELL: Thermal/residual stress in an electron beam physical vapor deposited thermal barrier coating system. *Acta Materialia*, **46**(1998)16, 5839-5850.

[8] H. LAU, C. LEYENS, U. SSCHULZ, C. FRIEDRICH: Influence of bond coat pre-treatment and surface topology on the lifetime of EB-PVD TBCs. *Surface and Coatings Technology*, **165**(2003), 217-223.

[9] V.K. TOLPYGO, D.R. CLARKE, K.S. MURPHY: Oxidation-induced failure of EB-PVD thermal barrier coatings. *Surface and Coatings Technology*, **146-147**(2001), 124-131.

[10] J. LIU, J.W. BYEON, Y.H. SOHN: Effects of phase constituents/microstructure of thermally grown oxide on the failure of EB-PVD thermal barrier coating with NiCoCrAlY bond coat. *Surface and Coatings Technology*, **200**(2006)20-21, 5869-5876.

[11] B.A. PINT, K.L. MORE: Characterization of alumina interfaces in TBC systems. *Journal of Materials Science*, **44**(2009), 1676-1686.

[12] S.G. TERRY, J.R. LITTY and C.G. LEVI: Evolution of porosity and texture. In Thermal barrier coatings grown by EB-PVD, elevated temperature coatings: science and technology III, The Minerals, Metals and Materials Society, Warrendale, PA, (1999), 13-26.

[13] Y-Ch. JUNG, T. SASAKI, T. TOMIMATSU: Distribution and structures of nanopores in YSZ-TBC deposited by EB-PVD. *Science and Technology of Advanced Materials*, **4**(2013), 571-574.

[14] A.M. LIMARGA, D.R. CLARKE: Characterization of electron beam physical vapor-deposited thermal barrier coatings using diffuse optical reflectance. *International Journal of Applied Ceramic Technology*, **6**(2009)3, 400-409.

[15] M. Kelly, J. Singh, J. Todd, S. Copley, D. Wolfe: Metallographic techniques for evaluation of thermal barrier coatings produced by electron beam physical vapor deposition. *Materials Characterization*, **59**(2008), 863-870.

[16] S.M. MEIER, D.K. GUPTA: The evolution of thermal barrier coatings in gas turbine engine applications. *Journal of Engineering for Gas Turbines and Power*, **116**(1994)1, 250-257.
[17] A. SCRIVANI, G. RIZZI, U. BARDI, C. GIOLLI, M. MUNIZ MIRANDA, S. CIATTINI, A. FOSATTI, F. BORGIOLI: Thermal fatigue behavior of thick and porous thermal barrier coatings systems. *Journal of Thermal Spray Technology*, **16**(2007)5-6, 816-821.
[18] N. MARKOCSAN, P. NYLÉN, J. WIGREN: Low thermal conductivity coatings for gas turbine applications. *Journal of Thermal Spray Technology*, **16**(2007)4, 498-505.
[19] M. GÓRAL, M. DRAJEWICZ, M. PYTEL, S. KOTOWSKI: Characterization of powders used for LPPS Thin Film plasma spraying of thermal barrier coatings. *Journal of Achievements in Materials and Manufacturing Engineering*, **47**(2011)2, 157-165.
[20] J. SZALA: MeTilo v.12.1 – instruction manual, University ..., Katowice 2009 (unpublished).
[21] G. MOSKAL: The porosity assessment of thermal barrier coatings obtained by APS method. *Journal of Achievements in Materials and Manufacturing Engineering*, **20**(2007)1-2, 483-486.

Received in February 2016